Inorganic Chemistry

Article

pubs.acs.org/IC

Solid-State and Solution-State Coordination Chemistry of Lanthanide(III) Complexes with (Pyrazol-1-yl)acetic Acid

Xiao-Yan Chen,[†] George S. Goff,*[,†] Brian L. Scott,[‡] Michael T. Janicke,[†] and Wolfgang Runde*[,§]

[†]Chemistry Division, [‡]Material Physics and Applications Division, and [§]Science Program Office, Los Alamos National Laboratory, Los Alamos, New Mexico 87545, United States

Supporting Information

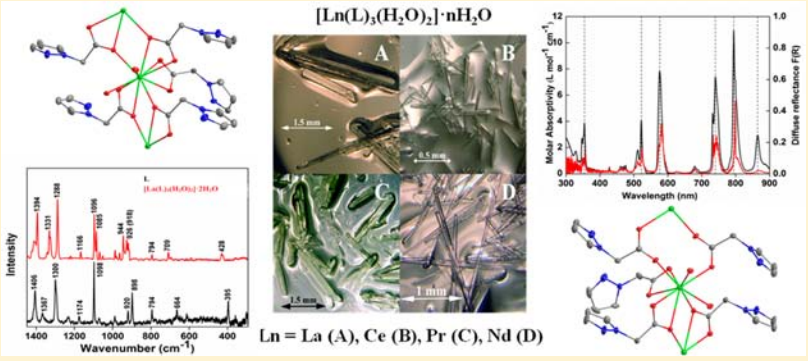

ABSTRACT: As a precursor of carboxyl-functionalized task-specific ionic liquids (TSILs) for f-element separations, (pyrazol-1-yl)acetic acid (**L**) can be deprotonated as a functionalized pyrazolate anion to coordinate with hard metal cations. However, the coordination chemistry of **L** with f-elements remains unexplored. We reacted **L** with lanthanides in aqueous solution at pH = 5 and synthesized four lanthanide complexes of general formula $[Ln(L)_3(H_2O)_2]\cdot nH_2O$ (**1**, Ln = La, n = 2; **2**, Ln = Ce, n = 2; **3**, Ln = Pr, n = 2; **4**, Ln = Nd, n = 1). All complexes were characterized by single crystal X-ray diffraction analysis revealing one-dimensional chain formations. Two distinct crystallographic structures are governed by the different coordination modes of carboxylate groups in **L**: terminal bidentate and bridging tridentate (**1**−**3**); terminal bidentate, bridging bidentate, and tridentate coordination in **4**. Comparison of the solid state UV−vis−NIR diffuse reflectance spectra with solution state UV−vis−NIR spectra suggests a different species in solution and solid state. The different coordination in solid state and solution was verified by distinctive ^{13}C NMR signals of the carboxylate groups in the solid state NMR.

INTRODUCTION

Pyrazole derivatives have attracted great attention due to the various biological properties of the pyrazole heterocycle, such as antipyretic,[1] analgesic,[1] antiinflammatory,[2] antitubercular,[3] antimicrobial,[3−5] anticancer,[6,7] etc. The potential of pyrazole−metal complexes for pharmaceutical applications has been recognized,[8] and the first pyrazole complex, *cis*-dichlorobis-(pyrazole)platinum(II), with cancer-targeting abilities was reported in 2000.[9] Since then, pyrazole-based compounds complexed with palladium, platinum, copper, gold, zinc, cobalt, nickel, iron, silver, and gallium have been investigated for therapeutic drug development.[8] In contrast to transition metals, fewer studies have been reported on lanthanide pyrazole compounds[10−21] despite the fact that lanthanide elements are increasingly used in industrial, technological, and medical applications.[22−27]

Pyrazole is a five-membered heterocyclic aromatic ring consisting of three carbon atoms and two adjacent N atoms. One of the pyrazole N atoms is less basic than the N atom with a lone pair in the sp^2 orbital (pK_a = 11.5 and 14).[28] Tautomerism exists in pyrazole and symmetrically substituted pyrazoles, but substitution at the acidic N excludes the possibility of forming structural isomers.

The coordination chemistry of pyrazole is extremely rich, and over 20 coordination modes of pyrazole with transition metal cations have been reported.[29] In pyrazole complexes with hard Lewis bases such as trivalent lanthanides, mono- and polydentate, bridging and terminal coordination modes are observed.[10,11,18−21] Interestingly, the coordination of pyrazole to lanthanides only occurred at high temperature in the presence of mercury.[10,11,18−21] The acidity of the pyrazole ring can be increased by incorporating hard acidic functional groups, e.g., carboxyl groups. Crystal structures have only been reported for lanthanides with pyrazole-3,5-dicarboxylic acid[15−17] and 4-iodopyrazole-3,5-dicarboxylic acid[14] synthesized under hydrothermal conditions. Among the known complexes, 12 coordination modes were observed including terminal and bridging carboxylate groups or bridging and chelating pyrazole N and carboxylate groups. For pyrazole-3,5-dicarboxylic acid, two- and three-dimensional lanthanide(III) complexes were

Received: December 10, 2012
Published: March 4, 2013

   dx.doi.org/10.1021/ic302696m | *Inorg. Chem.* 2013, 52, 3217−3224

characterized with three different structural breaks observed across the Ln series.[16,17] A series of one- and three-dimensional heterometallic Cu−Ln polymers were reported with pyrazole-3,5-dicarboxylic acid.[15] For 4-iodopyrazole-3,5-dicarboxylic acid, dinuclear molecular structure and one-dimensional Cu−Ln complexes were characterized.[14]

Our research group has been developing task-specific ionic liquids (TSILs) with covalently tethered functional groups to dissolve f-elements for the separation and recycling of used nuclear fuel. Since previous studies show that pyrazolium ILs have better electrochemical windows than some other common ILs, such as imidazolium, sulfonium, or guanidinium ILs,[30−32] pyrazolium-based TSILs are promising compounds with wider electrochemical window for electrochemical applications. A potential candidate for inclusion into an ionic liquid is (pyrazol-1-yl)acetic acid (Scheme 1), which can be deprotonated as a

Scheme 1

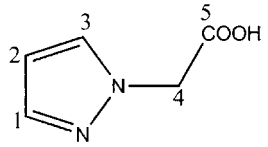

functionalized pyrazolate anion or undergo further substitution on the neutral N atom as a functionalized pyrazolium cation. Boa et al. first synthesized (pyrazol-1-yl)acetic acid in 2005, and reported that attempts to prepare first-row transition metal complexes had failed except for Cu(II).[33] It is not surprising that the coordination of (pyrazol-1-yl)acetic acid with lanthanides or actinides is rather unexplored, and it remains to be shown if (pyrazol-1-yl)acetic acid can be used as a TSIL precursor for lanthanide and actinide separations. In order to fill this knowledge gap, we reacted several lanthanides with (pyrazol-1-yl)acetic acid in aqueous solutions, isolating crystals which were structurally characterized by single crystal X-ray diffraction. Spectroscopic methods (UV−vis−NIR absorbance, diffuse reflectance spectra and ^{13}C NMR spectra) were also used to explore the coordination chemistry in solution and solid state.

EXPERIMENTAL METHODS

Pyrazole (98%) was used as received from Acros. All other chemicals were purchased from Fisher Scientific, Inc., and solutions were prepared with distilled deionized water (specific resistance ≥18.0 MΩ cm). (Pyrazol-1-yl)acetic acid (**L**) was prepared as described in the literature.[33] Stock solutions of **L** (0.5 M) were prepared gravimetrically by dissolving **L** in water with the pH adjusted to 5 by adding 1 M NaOH.

Lanthanide stock solutions were prepared by dissolving $Ln(NO_3)_3{\cdot}6H_2O$ (99.99% purity) in water. Four lanthanide(III) complexes (La (**1**), Ce (**2**), Pr (**3**), and Nd (**4**)) with **L** were prepared under mild conditions by adding 1 mL of 0.5 M Ln(III) nitrate stock to 3 mL of the **L** stock solution in a 20 mL borosilicate scintillation vial. The vial was capped, and crystallization of the lanthanide compounds occurred at room temperature within 3−5 days. During the crystallization, the solution pH remains constant at 5. Crystals of **1**−**4** were isolated, and their structures were determined by single crystal X-ray diffraction.

Crystals were removed from the solutions, mounted using a nylon cryoloop and Paratone-N oil, and cooled with a liquid nitrogen vapor stream. The data were collected on a Bruker D8 diffractometer, with an APEX II charge-coupled-device (CCD) detector, and a Bruker Kryoflex low temperature device. The instrument was equipped with a graphite monochromatized Mo Kα X-ray source (λ = 0.710 73 Å). A hemisphere of data was collected using ω scans, with 10-s frame exposures and 0.5° frame widths. Data collection and initial indexing and cell refinement were handled using APEX II software.[34] Frame integration, including Lorentz-polarization corrections, and final cell parameter calculations were carried out using SAINT+ software.[35] The data were corrected for absorption using redundant reflections and the SADABS program.[36] Decay of reflection intensity was not observed as monitored via analysis of redundant frames. The structure was solved using direct methods and difference Fourier techniques. Hydrogen atom positions were idealized on methyl and pyrazole rings, but were not refined on water molecules. The final refinement included anisotropic temperature factors on all non-hydrogen atoms. Structure solution, refinement, and creation of publication materials were performed using SHELXTL.[37]

Raman spectra of solid samples were collected with a Nicolet Magna-IR 560 ESD with a Raman accessory using a 1064 nm excitation laser to minimize fluorescence (which was observed for **L** when using a 780 nm laser). Diffuse reflectance spectra were measured for ground crystal samples using a Cary 5 UV−vis−NIR spectrophotometer with a diffuse reflectance attachment, while solution absorbance spectra were obtained by using a Cary 5 UV−vis−NIR spectrophotometer. Compound **1** was characterized by ^{13}C NMR spectroscopy in D_2O at room temperature on a Bruker ARX-300 spectrometer equipped with 5- and 10-mm multinuclear probes. The frequency was 75 MHz for the ^{13}C nuclei. The solid-state ^{13}C NMR spectroscopy of **1** was measured on Bruker AVANCE 400 MHz wide-bore solid-state NMR equipped with a 4 mm broadband Bruker Magic Angle Spinning probe.

RESULTS AND DISCUSSION

The reaction of four lanthanides with (pyrazol-1-yl)acetic acid (**L**) resulted in the formation of crystalline compounds with the general formula $[Ln(L)_3(H_2O)_2]{\cdot}nH_2O$ (**1** Ln = La, n = 2; **2** Ln = Ce, n = 2; **3** Ln = Pr, n = 2; **4** Ln = Nd, n = 1). Photographs of the crystals are shown in Figure 1.

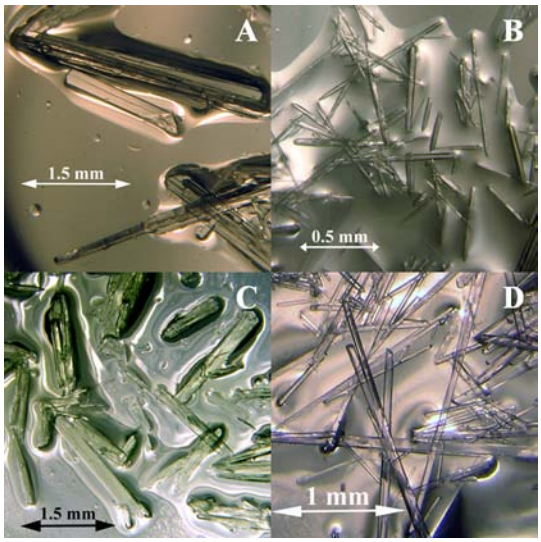

Figure 1. Photographs of single crystals $[Ln(L)_3(H_2O)_2]{\cdot}2H_2O$, Ln = La (A), Ce (B), Pr (C), and $[Nd(L)_3(H_2O)_2]{\cdot}H_2O$ (D).

Crystal Structures. Crystallographic analysis revealed the crystals to be $[La(L)_3(H_2O)_2]{\cdot}2H_2O$ (**1**), $[Ce(L)_3(H_2O)_2]{\cdot}2H_2O$ (**2**), $[Pr(L)_3(H_2O)_2]{\cdot}2H_2O$ (**3**), and $[Nd(L)_3(H_2O)_2]{\cdot}H_2O$ (**4**). Crystal data collection and refinement details for complexes **1**−**4** are listed in Table 1, while selected bond lengths and angles are given in Table 2.

dx.doi.org/10.1021/ic302696m | Inorg. Chem. 2013, 52, 3217−3224

Table 1. Selected Crystal Data and Structure Refinements for $[Ln(L)_3(H_2O)_2]\cdot nH_2O$ (Ln = La, Ce, Pr, n = 2; Ln = Nd, n = 1)

	1	2	3	4
T (K)	120(1)	120(1)	120(1)	140(1)
formula	$C_{15}H_{23}LaN_6O_{10}$	$C_{15}H_{23}CeN_6O_{10}$	$C_{15}H_{23}N_6O_{10}Pr$	$C_{15}H_{21}N_6NdO_9$
fw	586.30	587.51	588.30	573.62
cryst syst	monoclinic	monoclinic	monoclinic	monoclinic
space group	$P2_1/n$	$P2_1/n$	$P2_1/n$	$P2_1/n$
a (Å)	8.9380(6)	8.8937(5)	8.8744(5)	9.2686(7)
b (Å)	29.4106(18)	29.3072(18)	29.2893(17)	15.4688(12)
c (Å)	9.3713(6)	9.3379(6)	9.3719(6)	14.4631(12)
β (deg)	117.664(1)	117.433(1)	117.643(1)	99.963(1)
V (Å^3)	2181.8(2)	2160.2(2)	2157.9(2)	2042.4(3)
Z	4	4	4	4
ρ (g/cm^3)	1.785	1.806	1.811	1.866
μ (mm^{-1})	2.022	2.172	2.322	2.604
F(000)	1168	1172	1176	1140
crystal size (mm^3)	0.18 × 0.10 × 0.08	0.20 × 0.04 × 0.02	0.22 × 0.12 × 0.06	0.20 × 0.04 × 0.04
θ (deg)	2.55−28.35	2.55−28.51	2.55−28.39	1.94−28.31
index ranges	$-11 \le h \le 11$	$-11 \le h \le 11$	$-11 \le h \le 11$	$-12 \le h \le 12$
	$-39 \le k \le 38$	$-39 \le k \le 38$	$-37 \le k \le 37$	$-20 \le k \le 20$
	$-12 \le l \le 12$	$-11 \le l \le 12$	$-11 \le l \le 12$	$-19 \le l \le 19$
min and max transm	0.7123 and 0.8550	0.6705 and 0.9579	0.6290 and 0.8732	0.6240 and 0.9030
GOF on F^2	1.303	1.376	1.907	1.375
R_1, R_2 [$I > 2\sigma(I)$]	0.0270, 0.0645	0.0336, 0.0761	0.0249, 0.0603	0.0258, 0.0651
R_1, R_2 (all data)	0.0336, 0.0685	0.0434, 0.0805	0.0270, 0.0632	0.0345, 0.0676
largest diff. peak and hole (e Å^{-3})	0.830, −0.701	1.477, −0.772	0.862, −0.782	0.906, −0.756

Compared with the previously reported structures of lanthanides with pyrazole-3,5-dicarboxylic acid,[15−17] **L** only has one carboxyl group and the acetic acid is substituted directly to one of the N atom of the pyrazole ring. This substitution excludes the other N atom from chelating lanthanides, leading to the formation of one-dimensional chains for complexes **1**−**4** compared to the two- and three-dimensional networks previously reported in the literature. The different coordination modes of **L** observed in **1**−**3** (terminal bidentate and bridging tridentate) and **4** (terminal bidentate, bridging bidentate and tridentate) result in two distinct crystallographic structures.

*$[Ln(L)_3(H_2O)_2]\cdot 2H_2O$ (Ln = La (**1**), Ce (**2**), and Pr (**3**)).* Complexes **1**−**3** are isostructural, crystallizing in the monoclinic space group $P2_1/n$, with bridging ligands forming an extended one-dimensional chain. In the following, the structure of complex **1** is described as a representative example. The unit cell contains one unique La(III) center, three deprotonated ligands as monoanions, and two coordinated water molecules with two lattice water molecules. The metal to ligand ratio is 1:3. The thermal ellipsoid and atomic numbering scheme for the coordination environment around the La(III) ion is shown in Figure 2. The La(III) ion is 10-coordinate with two oxygen atoms from one terminal bidentate coordinated **L**, six oxygen atoms from four bridging tridentate coordinated **L**, and two coordinated water molecules. Four of the bridging oxygen atoms exhibit μ_3-coordination, and the La1−O1 and La1B−O1 bond lengths for the first two symmetric bridging ligands are 2.6840(17) and 2.5264(17) Å, respectively, which is more diverged than those with μ_3-oxygen atom in the three-dimensional La(III) pyrazole-3,5-dicarboxylate complex (2.554(6) and 2.585(5) Å).[16] The La1−O1−La1B bond angle is 116.85(7)°. The dihedral angle of the two neighboring rhombohedral planes defined by La1, O1, La1B, O1B and La1, O5, La1A, O5A is 34.25(9)°. In the first tridentate ligand, the La1−O2 bond length (2.6414(17) Å) is shorter than the La1−O1 bond length (2.6840(17) Å) with the bridging μ_3-oxygen atom. The C−O bond lengths of the carboxylate group are 1.240(3) and 1.278(3) Å, which suggest that there is some electron delocalization in the carboxylate groups compared with the C−O bond lengths of the carboxylate group in the free ligand (1.207(2) and 1.309(2) Å).[33] Within the first tridentate ligand, the least-squares planes of the pyrazole ring (N1, N2, C3, C4, and C5) and carboxylate group (C1, O1, and O2) are almost mutually perpendicular with a dihedral angle of 85.79(14)°, which is even larger than that of the free **L** (80.76(6)°). Such a twist can be explained by the higher steric hindrance from the coordination with the La(III) ion.

For the second set of tridentate **L**, the La1−O5 and La1A-O5 bond lengths for the μ_3-oxygen atoms are 2.4924(17) and 2.7720(17) Å, respectively, with a larger La1−O5−La1A bond angle of 118.25(6)° compared to the La1−O1−La1B angle. The difference between the two C−O bond lengths (1.247(3) and 1.267(3) Å) is even smaller indicating a greater degree of electron delocalization. For the bidentate terminal ligand, the carboxylate group has very similar C−O bond lengths (1.257(3) and 1.265(3) Å). The difference between these two C−O bond lengths is smaller than those in the tridentate **L**, which suggests a stronger electron delocalization in the carboxylate group in the bidentate **L**. The O3−La1−O4 bond angle is 49.84(5)° with La−O bond lengths of 2.5487(18) and 2.6723(18) Å, which are shorter than those in the La(III) pyrazole-3,5-dicarboxylate complex (2.585(5) and 2.906(7) Å)[16] indicating stronger bonding of the carboxylate group with La(III) in **1**. The dihedral angle of the least-squares planes of the pyrazole and carboxylate group in the bidentate **L** is 89.07(9)°, which is even larger than that in tridentate **L**. The two coordinated water molecules are *cis* to each other with an O7−La1−O8 angle of 68.39(6)°. Each La(III) ion is bridged to the neighboring La(III) ions by two tridentate **L** forming one-

dx.doi.org/10.1021/ic302696m | Inorg. Chem. 2013, 52, 3217−3224

Table 2. Selected Bond Lengths (Å) and Angles (deg) for 1−4

			$[La(L)_3(H_2O)_2]\cdot 2H_2O$ (**1**)		
Bond Lengths (Å)					
La1−O5	2.4924(17)	La1−O1	2.6840(17)	La1−O3	2.5487(18)
La1−O7	2.5619(17)	La1−O8	2.5851(19)	La1−O6	2.6048(17)
La1−O2	2.6414(17)	La1−O4	2.6723(18)	La1B−O1	2.5264(17)
La1A−O5	2.7720(17)	O2−C1	1.240(3)	O3−C6	1.257(3)
O5−C11	1.267(3)	O1−C1	1.278(3)	O4−C6	1.265(3)
O6−C11	1.247(3)				
Bond Angles (deg)					
O5−La1−O3	71.59(6)	O1−La1−O3	104.55(5)	O5−La1−O7	80.08(6)
O1−La1−O7	121.08(5)	O3−La1−O7	134.15(6)	O5−La1−O8	72.45(6)
O8−La1−C6	135.37(7)	O3−La1−O8	131.04(6)	O7−La1−O8	68.39(6)
O1−La1−O2	48.87(5)	O3−La1−O4	49.84(5)	O3−La1−O6	84.22(6)
La1−O1−La1B	116.85(7)	O2−C1−O1	122.1(2)	O3−C6−O4	121.7(2)
La1−O5−La1A	118.25(6)	O6−C11−O5	122.4(2)		
			$[Ce(L)_3(H_2O)_2]\cdot 2H_2O$ (**2**)		
Bond Lengths (Å)					
Ce1−O1	2.674(2)	Ce1−O5	2.779(2)	Ce1−O3	2.525(2)
Ce1−O7	2.536(2)	Ce1−O8	2.572(2)	Ce1−O6	2.579(2)
Ce1−O2	2.611(2)	Ce1−O4	2.663(2)	O3−C6	1.255(4)
O2−C1	1.242(4)	O1−C1	1.276(4)	O6−C11	1.243(4)
O5−C11	1.266(4)	O4−C6	1.264(4)		
Bond Angles (deg)					
O3−Ce1−O1	104.91(7)	O7−Ce1−O1	120.89(7)	O8−Ce1−O1	69.47(7)
O5−Ce1−O8	72.55(8)	O5−Ce1−O3	71.22(8)	O3−Ce1−O7	134.01(7)
O7−Ce1−O8	68.42(8)	O1−Ce1−O8	89.90(8)	O3−Ce1−O8	131.02(8)
O4−Ce1−C6	25.57(8)	O1−Ce1−O2	49.25(7)	O3−Ce1−O4	50.19(7)
O6−C11−O5	122.8(3)	O2−C1−O1	122.0(3)	O3 −C6-O4	122.0(3)
			$[Pr(L)_3(H_2O)_2]\cdot 2H_2O$ (**3**)		
Bond Lengths (Å)					
Pr1−O3	2.7927(16)	Pr1−O5	2.4796(16)	Pr1−O2	2.5092(17)
Pr1−O7	2.5157(17)	Pr1−O8	2.5500(18)	Pr1−O1	2.6384(16)
Pr1−O4	2.5573(16)	O3−C6	1.267(3)	O5−C11	1.275(3)
O1−C1	1.266(3)	O4−C6	1.244(3)	O6−C11	1.240(3)
Bond Angles (deg)					
O7−Pr1−O8	68.75(6)	O5−Pr1−O7	78.01(5)	O3−Pr1−O2	66.57(5)
O5−Pr1−O6	112.10(5)	O5−Pr1−O8	89.44(6)	O2−Pr1−O7	133.34(5)
O4−C6−O3	122.4(2)	O2−Pr1−O1	50.51(5)	O2−Pr1−O8	131.70(6)
O5−Pr1−O3	117.97(5)	O6−C11−O5	121.9(2)	O8−Pr1−O1	135.99(6)
O7−Pr1−O1	149.38(5)	O4−Pr1−O1	78.77(5)	O2−C1−O1	121.4(2)
			$[Nd(L)_3(H_2O)_2]\cdot H_2O$ (**4**)		
Bond Lengths (Å)					
Nd1−O5	2.365(2)	Nd1−O7	2.495(2)	Nd1−O4	2.547(2)
Nd1−O8	2.464(2)	Nd1−O3	2.581(2)	Nd1−O2	2.501(2)
Nd1−O1	2.705(2)	O3−C6	1.264(4)	O1−C1	1.274(3)
Nd1−O6	2.454(2)	O6−C11	1.249(4)	O4−C6	1.261(4)
Nd1B−O1	2.459(2)	O2−C1	1.243(3)		
Bond Angles (deg)					
O5−Nd1−O8	137.51(7)	O4−Nd1−O3	51.11(6)	O5−Nd1−O3	72.25(7)
O5−Nd1−O7	70.30(7)	O1−Nd1−O2	49.82(6)	O4−Nd1−O8	140.02(7)
O8−Nd1−O7	67.58(7)	O8−Nd1−O3	142.15(7)	O7−Nd1−O3	128.18(7)
O3−Nd1−O1	117.80(6)	O5−Nd1−O1	122.04(7)	O5−Nd1−O2	75.60(7)
O1−C1−O2	121.9(3)	O3−C6−O4	122.4(3)	O6−C11−O5	124.4(3)

dimensional chains along the *a*-axis, shown in Figure 3, with the La···La distances alternating between 4.5209(4) and 4.4397(4) Å.

*$[Nd(L)_3(H_2O)_2]\cdot H_2O$ (**4**).* Complex **4** also contains one-dimensional chains and crystallizes in the monoclinic space group $P2_1/n$. The unit cell contains one unique Nd(III) center, three deprotonated ligands as monoanions, and two coordinated water molecules with only one lattice water molecule. The Nd(III) ion is nine-coordinate with seven oxygen atoms from five ligands and two oxygen atoms from coordinated water molecules (Figure 4). In addition to the terminal bidentate and bridging tridentate modes of **L** found in **1**−**3**, a third coordination mode of bidentate bridging is present in **4**. The tridentate bridging **L** links Nd1 and Nd1B with a distance of

dx.doi.org/10.1021/ic302696m | *Inorg. Chem.* 2013, 52, 3217−3224

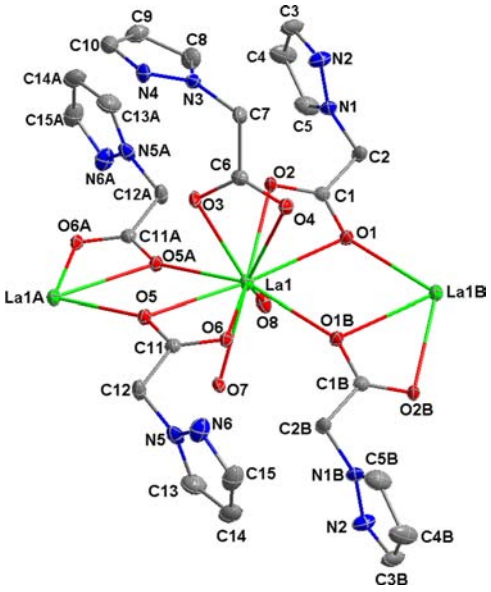

Figure 2. Thermal ellipsoids (50% probability) of $[La(L)_3(H_2O)_2]\cdot 2H_2O$ (**1**). The hydrogen atoms and the lattice water molecules have been removed for clarity.

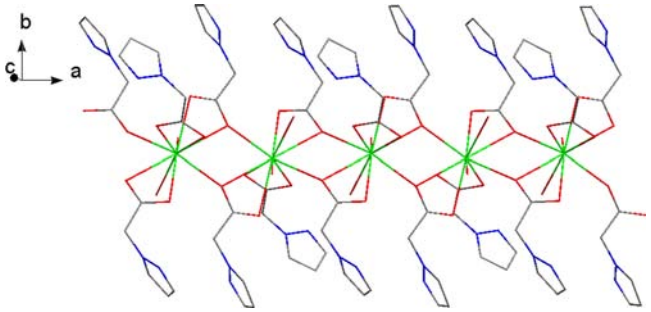

Figure 3. One-dimensional chain of $[La(L)_3(H_2O)_2]\cdot 2H_2O$ (**1**): La, green; C, gray; O, red; N, blue. The hydrogen atoms and the lattice water molecules have been removed for clarity.

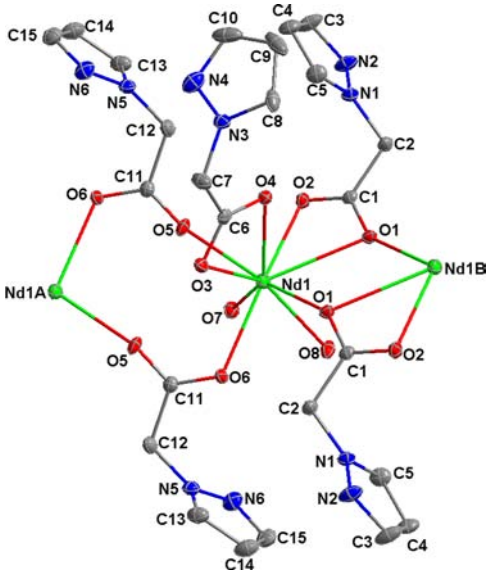

Figure 4. Thermal ellipsoids (50% probability) of $[Nd(L)_3(H_2O)_2]\cdot H_2O$ (**4**). The hydrogen atoms and the lattice water molecules have been removed for clarity.

4.3789(4) Å, which is smaller than the La···La distance in **1**. A significantly shorter Nd1−O2 bond length (2.501(2) Å) is observed for the tridentate ligand compared to the La−O bonds found in **1** (2.6414(17) Å). The bond length of μ_3-oxygen atom O1 with Nd1 (2.705(2) Å) is longer than that in **1** (La1−O1, 2.6840(17) Å). The difference between the Nd1−O1 (2.705(2) Å) and Nd1B−O1 (2.459(2) Å) bond lengths with the μ_3-oxygen atom is also larger than that in the three-dimensional Nd(III) complex with pyrazole-3,5-dicarboxylic acid (2.437(3) and 2.640(3) Å).[17] A smaller dihedral angle of 79.68(12)° between the least-squares planes of the pyrazole (N1, N2, C3, C4, and C5) and carboxylate group (C1, O1 and O2) for the tridentate **L** is observed compared with those of **1** (85.79(14)° and 89.07(9)°) and free ligand (80.76(6)°).[33] For the bidentate bridging **L**, the carboxylate group bridges the Nd1 and Nd1A with the Nd−O bond lengths of 2.365(2) and 2.454(2) Å. The resulting Nd1···Nd1A distance of 4.9784(4) Å represents the longest Ln···Ln distances among the four complexes reported here. The least-squares planes of the pyrazole and carboxylate group of the bidentate bridging **L** show a larger dihedral angle of 82.82(11)° compared to that in the tridentate ligand. The difference between the two C−O bond lengths in a single carboxylate group of **L** decreases in the following order: tridentate bridging (0.031 Å) > bidentate bridging (0.005 Å) > terminal bidentate (0.002 Å). Such a trend indicates the strongest electron delocalization occurs in the carboxylate group of the terminal bidentate **L**, as observed in **1**. The alternate tridentate and bidentate bridging **L** links neighboring Nd(III) ions to form a one-dimensional chain structure (Figure 5).

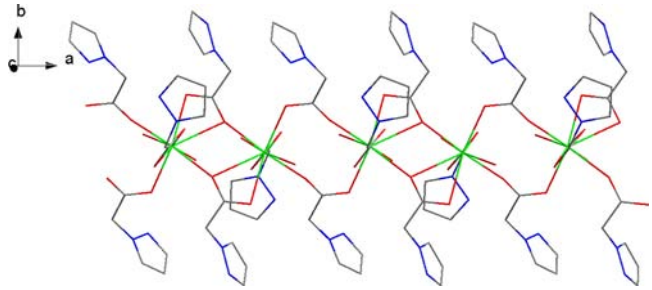

Figure 5. One-dimensional chain of $[Nd(L)_3(H_2O)_2]\cdot H_2O$ (**4**): Nd, green; C, gray; O, red; N, blue. The hydrogen atoms and the lattice water molecules have been removed for clarity.

The change in coordination mode in complex **4** can be explained by the lanthanide contraction. Although La, Ce, Pr, and Nd are all considered light lanthanides, single crystal X-ray analysis reveals a structural break between Pr (**3**) and Nd (**4**). As shown in Figure 6, the average Ln−O bond lengths of the terminal bidentate **L** and coordinated water molecules decrease with decreasing ionic radii[38] caused by the well-known lanthanide contraction.[39] For the carboxylate group in the tridentate bridging **L**, the Ln−O6 bond lengths decrease while the Ln−O5 (μ_3-bridging oxygen) bond lengths increase. Due to the smaller ionic radii of the Nd(III) ion the Nd−O6 bond is significantly shortened accompanied with the breakage of the Nd−O5 bond resulting in the coordination mode change of the second bridging ligand from tridentate bridging to bidentate bridging. This change in coordination results in a one-dimensional chain of alternating tridentate and bidentate bridging ligands (Figure 5).

dx.doi.org/10.1021/ic302696m | Inorg. Chem. 2013, 52, 3217−3224

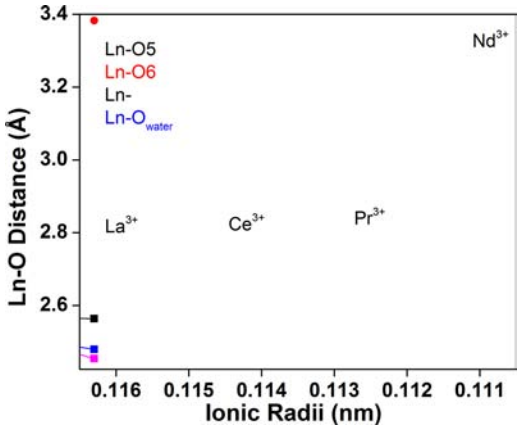

Figure 6. Comparison of the average Ln−O bond lengths with decreasing ionic radii: Ln−$O_{bidentate}$, black; Ln−O5, red; Ln−O6, purple; Ln−O_{water}, blue; Nd···O5, red dot. Ionic radii for 9- and 10-coordinate lanthanide cations were taken from Shannon et al.[38]

Spectroscopic Characterization. *Solid-State FT-Raman Spectroscopy.* To date, there is no Raman spectroscopy study reported for (pyrazol-1-yl)acetic acid. The solid-state FT-Raman spectra for all the compounds we synthesized are very similar (**1** is shown in Figure 7 as an example). The C═O

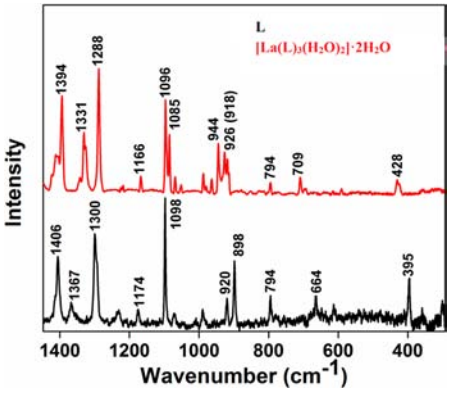

Figure 7. Solid-state FT-Raman spectra of $[La(L)_3(H_2O)_2]\cdot 2H_2O$ (**1**) (red) and **L** (black).

stretching mode is not observed in the FT-Raman spectra. A similar case has been previously published.[40] The C−O symmetric and asymmetric stretching modes are observed at 1300 and 1174 cm^{-1} for the free ligand, which shifted to lower frequencies of 1288 and 1166 cm^{-1} upon coordination with La(III). The weak peak at 1367 cm^{-1} in the free ligand can be assigned as either pyrazole ring stretching mode or δ(C−OH) bending mode, which shifts to lower frequency at 1331 cm^{-1} with increased intensity in **1**.[41] Similar peak shifts and intensity changes have been reported for the lanthanide complexes with 3,5-pyrazoledicarboxylic acid.[42] Medium-strong to strong peaks at 1406 and 1098 cm^{-1} in the free ligand are due to the pyrazole ring stretching modes.[42] In **1**, these ring stretching peaks also shift to lower frequencies (1394 and 1096 cm^{-1}) with extra shoulder peaks caused by the existence of two different ligands in the complex. Similar peak shifts and splitting can be seen for the pyrazole ring bending mode at 920 and 898 cm^{-1} in the free ligand and multiple peaks around 944 and 926 cm^{-1} in the La(III) complex. The weak Raman band at 794 cm^{-1} is attributed to the δ(CH) bending mode, which is unchanged in the complex. The band at 664 cm^{-1} for the bending mode of δ(O═CO) shifts to higher frequency at 709 cm^{-1} in complex **1**. The medium peak of 395 cm^{-1} in the Raman spectrum of the ligand might be the bending mode of the pyrazole ring.[43] In the low wavenumber region of the complex, we observed a weak band at 428 cm^{-1} with a shoulder at 424 cm^{-1}, which might be a combination of the ring bending modes and the new La−O vibration mode.[42]

The Raman bands at 3144−3119 cm^{-1} are assigned to stretching modes of ν(CH) (see Supporting Information). The symmetric and asymmetric stretching modes of CH_2 are observed at 2956 and 2990 cm^{-1}. The Raman spectra of all the complexes show broad peaks at 3350−3450 cm^{-1} (see Supporting Information), which belong to the vibrational stretches of water molecules in the complexes.

Solution UV−Vis−NIR Spectroscopy and UV−Vis−NIR Diffuse Reflectance. $[Pr(L)_3(H_2O)_2]\cdot 2H_2O$ (**3**) and $[Nd(L)_3(H_2O)_2]\cdot H_2O$ (**4**) were characterized by solid-state diffuse reflectance spectroscopy. After dissolving all four solid compounds in water (pH = 5), the UV−vis−NIR absorbances were measured to assess coordination modes in solution. The UV absorption spectrum of **L** shows one $\pi-\pi^*$ absorption peak at (λ_{max} = 217 nm) (see Supporting Information), which is almost the same as the absorption of pyrazole.[44] The molar absorption coefficient of **L** at 217 nm is 5.47 × 10^3 L mol^{-1} cm^{-1}, which is much higher than that of pyrazole (1.2 × 10^3 L mol^{-1} cm^{-1}).[44] All spectra of the dissolved complexes show this absorption at 217 nm with the molar absorption coefficient around 10^4 L mol^{-1} cm^{-1} (**1**, 1.73 × 10^4; **2**, 1.762 × 10^4, **3**, 1.95 × 10^4; **4**, 1.64 × 10^4 L mol^{-1} cm^{-1}), which is nearly three times that of the free ligand. The increased molar absorption coefficient of the solution species compared to the free ligand precursor matches the 3:1 metal to ligand ratio in the solid state by the X-ray diffraction analysis.

The solution state UV−vis−NIR absorbances of **3** and **4** are characterized by a number of Laporte-forbidden f−f transitions above 300 nm.[45,46] The solution UV−vis−NIR spectra and the molar absorptivities show general agreement with the characteristic f−f transitions for the Ln(III) aquo ion absorbance (Figures 8 and 9). The complexation of the Ln(III) ions with **L** results in only very small shifts of the most prominent absorbance bands. For complex **3**, the characteristic transitions are observed at 444.2, 468.6, 481.9, and 589.7 nm, which compares well to 444, 468, 481, and 589 nm ($^3H_4 \rightarrow {}^3P_2$, $^3P_1$, $^3P_0$, $^1D_2$) for Pr^{3+}(aq) in dilute perchloric acid.[45−47] The molar

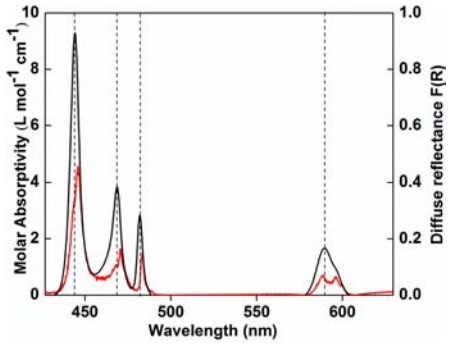

Figure 8. Solution state UV−vis−NIR spectrum (black) and solid state UV−vis−NIR diffuse reflectance spectrum (red) of $[Pr(L)_3(H_2O)_2]\cdot 2H_2O$ (**3**) dissolved in H_2O. The Pr^{3+}(aq) absorbance peaks in diluted perchloric acid are shown as dotted lines.[45]

dx.doi.org/10.1021/ic302696m | Inorg. Chem. 2013, 52, 3217−3224

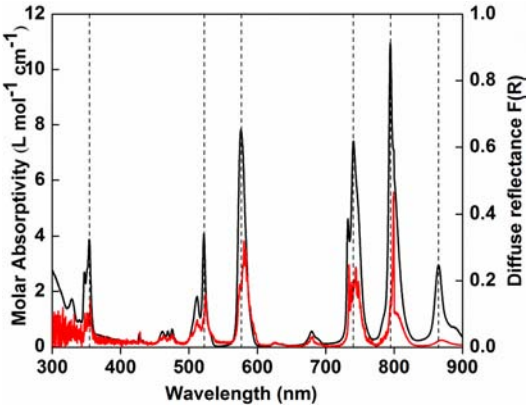

Figure 9. Solution state UV−vis−NIR spectrum (black) and solid state UV−vis−NIR diffuse reflectance spectrum (red) of $[Nd(L)_3(H_2O)_2]\cdot H_2O$ (**4**). The Nd^{3+}(aq) absorbance peaks in diluted perchloric acid are shown as dotted lines.[45]

absorptivity of 9.3 L mol^{-1} cm^{-1} at 444 nm for **3** is comparable to that reported for Pr^{3+} aquo ion in dilute perchloric acid (11 L mol^{-1} cm^{-1}).[45] Similarly, the primary absorbance peaks of dissolved $[Nd(L)_3(H_2O)_2]\cdot H_2O$ (**4**) (Figure 9) are observed at 347, 355, 512.5, 522.3, 575.5, 732.5, 740.8, 794.9, and 864.2 nm ($^4I_{9/2} \rightarrow {}^4D_{1/2}$, $^4D_{5/2}$, $^4D_{3/2}$, $^4G_{9/2}$, $^4G_{7/2}$, $^4G_{5/2}$, $^4S_{3/2}$, $^4F_{7/2}$, $^2H_{9/2}$), which correspond to the reported Nd^{3+}(aq) ion f−f transitions at 350, 353, 512, 521, 576, 732, 740, 802, and 865 nm.[45,46] The peak shifts and splitting are evidence for the coordination of Nd(III) with **L**. The molar absorptivity of **4** (7.29 L mol^{-1} cm^{-1}) at 578 nm is also slightly higher than that of Nd^{3+} aquo ion in diluted perchloric acid (5.8 L mol^{-1} cm^{-1}).[45] For complexes **3** and **4**, the solid state UV−vis−NIR diffuse reflectance spectra do not match their solution state UV−vis−NIR spectra suggesting different coordination environments around the lanthanide in solution and solid state. Both relative intensity ratios and peak shapes differ in the solution and solid state spectra. A maximum of 2 and 4 nm peak shift was observed in **3** and **4**, respectively.

^{13}C NMR Spectroscopy. We used ^{13}C NMR spectroscopy to explore the speciation and coordination modes in solution state and solid state. The free ligand (Scheme 1) shows five ^{13}C NMR signals at 52.24 ppm (C4), 106.61 (C2), 132.90 (C1), 139.81 (C3), and 172.23 (C5) ppm. The ^{13}C NMR spectrum of the diamagnetic La(III) complex dissolved in D_2O (pH = 5) displays the same ^{13}C NMR features but shifted from those of the free ligand. When **L** is chelating a metal ion, the carbon atoms of the COOH group are deshielded, illustrated as coordination-induced shifts, $\Delta\delta$. The $\Delta\delta$ value of 4.08 ppm (COOH) for the La(III) solution complex (Table 3) indicates that the carboxyl groups of the ligand are coordinated with the La(III) ions. All coordinated ligands in the La(III) solution complex are equivalent (Table 3) suggesting that only one solution La(III) species exists in solution. The absence of NMR shifts from the uncomplexed ligand indicates that all ligands are bound to La(III) in solution. The solid state ^{13}C NMR spectrum of complex **1** shows three distinct signals for the carboxyl groups (C5) (183, 181, 178 ppm) indicating the existence of three different bonding environments for **L**, which matches the crystal structure of **1**−**3** with two different tridentate bridging ligands and a single terminal bidentate ligand. From the crystal structure analysis, the bidentate ligand is the least deshielded, which shifts the ^{13}C signal to 178 ppm. The remaining two chemical shifts of 181 and 183 ppm are too close to distinguish between the two tridentate ligands. The three chemical shifts of C5 in the solid state are quite different from the single chemical shift of C5 at 176.31 ppm in solution ^{13}C NMR spectrum of **1**. The ^{13}C NMR shifts provide that there are three different ligands in the solid state while all the ligands in the solution state are the same, indicating different speciation in solid and solution state.

Table 3. ^{13}C NMR Chemical Shifts (δ, ppm) for the Free Ligand ((Pyrazol-1-yl)acetic acid) and $[La(L)_3(H_2O)_2]\cdot 2H_2O$ (1) Dissolved in D_2O and in Solid State

	C1	C2	C3	C4	C5
ligand (pH = 5)	132.90	106.61	139.81	52.24	172.23
complex **1** in D_2O (pH = 5)	132.02	105.99	139.79	54.37	176.31
complex **1** (solid state)	132	106	138	55	183, 181, 178

CONCLUSION

We have synthesized at room temperature and characterized four novel lanthanide complexes with (pyrazol-1-yl)acetic acid (**L**) of general formula $[Ln(L)_3(H_2O)_2]\cdot nH_2O$ (**1**, Ln = La, *n* = 2; **2**, Ln = Ce, *n* = 2; **3**, Ln = Pr, *n* = 2; **4**, Ln = Nd, *n* = 1). All of the complexes reveal a one-dimensional chain structure with tridentate and bidentate bridging ligands connecting adjacent lanthanide centers along the *a*-axis; however, two different structure types are found with the structural break occurring between Pr(III) and Nd(III). In addition to terminal bidentate and bridging tridentate ligands found in **1**−**3**, a third coordination mode (bidentate bridging) is observed in **4**, which is likely caused by the smaller ionic radii of the Nd(III) ion. The change of tridentate bridging to bidentate bridging mode also decreases the coordination number of the Ln(III) atom from 10 in **1**−**3** to 9 in **4**.

The spectroscopic characterization of solid state and solution compounds supports the different coordination environment found in the structural analysis. The shifts and intensity changes of the solid state UV−vis−NIR diffuse reflectance spectra from the solution state UV−vis−NIR spectra suggest a different species in solution and solid state. This was further verified by ^{13}C NMR studies of solution and solid state compounds. A single set of ligand NMR shifts different from those for the free ligand in solution suggests a single Ln(III)−ligand solution complex. The chemical shifts of carboxyl groups in the solid state ^{13}C NMR spectrum of **1** are observed at 183, 181, and 178 ppm, which are quite different from the single carboxyl group chemical shift at 176.31 ppm in the solution ^{13}C NMR spectrum; however, the three distinctive shifts for the different carboxyl groups match the single crystal X-ray analysis. The comparison of solution and solid state ^{13}C NMR spectra suggests that the lanthanide polymer chain breaks down in solution to form a different Ln(III) species in solution. Both NMR and vibrational spectroscopic data clearly identify that carboxyl groups of the ligand participate in the Ln(III) bonding. This research provides for the first time details of the structure and bonding of lanthanide complexes with (pyrazol-1-yl)acetic acid. As our first step toward developing TSILs, this information aids our development of deprotonated (pyrazol-1-yl)acetic acid as anion or N-substituted (pyrazol-1-yl)acetic

dx.doi.org/10.1021/ic302696m | Inorg. Chem. 2013, 52, 3217−3224

acid as cation in new TSILs for recycling of trivalent f-elements in used nuclear fuel.

■ ASSOCIATED CONTENT

Supporting Information

Crystallographic and spectroscopic data for the additional lanthanide complexes as described in the text. This material is available free of charge via the Internet at http://pubs.acs.org.

■ AUTHOR INFORMATION

Corresponding Author

*E-mail: georgeg@lanl.gov (G.S.G.), runde@lanl.gov (W.R.).

Notes

The authors declare no competing financial interest.

■ ACKNOWLEDGMENTS

The authors gratefully acknowledge the Los Alamos Laboratory Directed Research and Development Program and the G. T. Seaborg Institute for Transactinium Science at Los Alamos National Laboratory for financial support during this project.

■ REFERENCES

(1) Rainer, G.; Riedel, R.; Dittmann, E. C. *Fed. Rep. Ger.* **1976**, 23.
(2) Matsuda, H.; Morikawa, T.; Ando, S.; Iwao, T.; Masayuki, Y. *Bioorg. Med. Chem.* **2003**, *11*, 1995.
(3) Mor, S.; Mohil, R.; Kumar, D.; Ahuja, M. *Med. Chem. Res.* **2012**, *21*, 3541.
(4) Yadav, A. G.; Patil, V. N.; Asrondkar, A. L.; Naik, A. A.; Ansulkar, P. V.; Bobade, A. S.; Chowdhary, A. S. *Rasayan J. Chem.* **2012**, *5*, 117.
(5) Dias, H. V. R.; Batdorf, K. H.; Fianchini, M.; Diyabalanage, H. V. K.; Carnahan, S.; Mulcahy, R.; Rabiee, A.; Nelson, K.; van Waasbergen, L. G. *J. Inorg. Biochem.* **2006**, *100*, 158.
(6) Insuasty, B.; Tigreros, A.; Orozco, F.; Quiroga, J.; Abonia, R.; Nogueras, M.; Sanchez, A.; Cobo, J. *Bioorg. Med. Chem.* **2010**, *18*, 4965.
(7) Pal, D.; Saha, S.; Singh, S. *Int. J. Pharm. Pharm. Sci.* **2012**, *4*, 98.
(8) Keter, F. K.; Darkwa, J. *BioMetals* **2012**, *25*, 9.
(9) Sakai, K.; Tomita, Y.; Ue, T.; Goshima, K.; Ohminato, M.; Tsubomura, T.; Matsumoto, K.; Ohmura, K.; Kawakami, K. *Inorg. Chim. Acta* **2000**, *297*, 64.
(10) Deacon, G. B.; Junk, P. C.; Urbatsch, A. *Aust. J. Chem.* **2012**, *65*, 802.
(11) Viciano-Chumillas, M.; Tanase, S.; de Jongh, L. J.; Reedijk, J. *Eur. J. Inorg. Chem.* **2010**, 3403.
(12) Shi, X.-M.; Tang, R.-R.; Gu, G.-L.; Huang, K.-L. *Spectrochim. Acta, Part A* **2009**, *72*, 198.
(13) Montgomery, C. P.; New, E. J.; Palsson, L. O.; Parker, D.; Batsanov, A. S.; Lamarque, L. *Helv. Chim. Acta* **2009**, *92*, 2186.
(14) Zhou, X.-H.; Peng, Y.-H.; Gu, Z.-G.; Zuo, J.-L.; You, X.-Z. *Inorg. Chim. Acta* **2009**, *362*, 3447.
(15) Zhou, X.-H.; Peng, Y.-H.; Du, X.-D.; Wang, C.-F.; Zuo, J.-L.; You, X.-Z. *Cryst. Growth Des.* **2009**, *9*, 1028.
(16) Zhao, J.; Long, L.-S.; Huang, R.-B.; Zheng, L.-S. *Dalton Trans.* **2008**, 4714.
(17) Xia, J.; Zhao, B.; Wang, H.-S.; Shi, W.; Ma, Y.; Song, H.-B.; Cheng, P.; Liao, D.-Z.; Yan, S.-P. *Inorg. Chem.* **2007**, *46*, 3450.
(18) Kawahata, R.; Tsukuda, T.; Yagi, T.; Fuyuhiro, A.; Kaizaki, S. *J. Alloys Compd.* **2006**, *408*−*412*, 976.
(19) Deacon, G. B.; Forsyth, C. M.; Gitlits, A.; Skelton, B. W.; White, A. H. *Dalton Trans.* **2004**, 1239.
(20) Quitmann, C. C.; Bezugly, V.; Wagner, F. R.; Müller-Buschbaum, K. *Z. Anorg. Allg. Chem.* **2006**, *632*, 1173.
(21) Deacon, G. B.; Gitlits, A.; Skelton, B. W.; White, A. H. *Chem. Commun.* **1999**, 1213.
(22) Xu, W.; Kattel, K.; Park, J. Y.; Chang, Y.; Kim, T. J.; Lee, G. H. *Phys. Chem. Chem. Phys.* **2012**, *14*, 12687.
(23) Deng, W.; Goldys, E. M. *Langmuir* **2012**, *28*, 10152.
(24) Liu, C.; Zhang, L.; Zheng, Q.; Luo, F.; Xu, Y.; Weng, W. *Sci. Adv. Mater.* **2012**, *4*, 1.
(25) Vidaud, C.; Bourgeois, D.; Meyer, D. *Chem. Res. Toxicol.* **2012**, *25*, 1161.
(26) Dissanayake, P.; Averill, D. J.; Allen, M. J. *Sci. Synth., Knowl. Updates* **2011**, 1.
(27) Charbonniere, L. J. *Curr. Inorg. Chem.* **2011**, *1*, 2.
(28) Eicher, T.; Haputmann, S.; Suschitzky, H. *The Chemistry of Heterocycles: Structure, Reactions, Syntheses and Applications*; John Wiley & Sons: New York, 2003.
(29) Halcrow, M. A. *Dalton Trans.* **2009**, 2059.
(30) Caja, J.; Dunstan, T. D. J.; Katovic, V. *Proc. Electrochem. Soc.* **2002**, *19*, 1014.
(31) Abu-Lebdeh, Y.; Abouimrane, A.; Alarco, P.-J.; Armand, M. *J. Power Sources* **2006**, *154*, 255.
(32) Chai, M.; Jin, Y.; Fang, S.; Yang, L.; Hirano, S.-i.; Tachibana, K. *Electrochim. Acta* **2012**, *66*, 67.
(33) Boa, A. N.; Crane, J. D.; Kowalczyk, R. M.; Sultana, N. H. *Eur. J. Inorg. Chem.* **2005**, 872.
(34) *APEX II*; Bruker AXS. Inc.: Madison, WI, 2004.
(35) *SAINT+*; Bruker AXS. Inc.: Madison, WI, 2003.
(36) Sheldrick, G. *SADABS*; University of Gottingen: Gottingen, Germany, 2001.
(37) *SHELXTL*; Bruker AXS, Inc.: Madison, WI, 1997.
(38) Shannon, R. D. *Acta Crystallogr.* **1976**, *A32*, 751.
(39) Moeller, T. *The Chemistry of the Lanthanides*; Pergamon Press: Oxford, 1973.
(40) Bright, A.; Devi, T. S. R.; Gunasekaran, S. *Int. J. ChemTech Res.* **2010**, *2*, 379.
(41) Udaya, S. N.; Chaitanya, K.; Prasad, M. V. S.; Veeraiah, V.; Veeraiah, A. *J. Mol. Struct.* **2012**, *1019*, 68.
(42) Kostova, I.; Rastogi, V. K.; Kiefer, W. *J. Optoelectron. Adv. Mater.* **2008**, *10*, 1345.
(43) Sundaraganesan, N.; Kavitha, E.; Sebastian, S.; Cornard, J. P.; Martel, M. *Spectrochim. Acta, Part A* **2009**, *74A*, 788.
(44) Habibi, K. S. M.; Maghsoodlou, M. T.; Ebrahimi, A.; Zakarianejad, M.; Fattahi, M. *J. Solution Chem.* **2007**, *36*, 1117.
(45) Carnall, W. T. The Absorption and Fluoresence Spectra of Rare Earth Ions in Solution. In *Handbook on the Chemistry and Physics of the Rare Earths*; Gschneider, K. A., Jr., Eyring, L., Eds.; North-Holland Publishing Company: Amsterdam,1979; Chapter 24, pp 171−208.
(46) Carnall, W. T.; Fields, P. R.; Rajnak, J. *J. Chem. Phys.* **1968**, *48*, 4424.
(47) Kyômen, T.; Sakamoto, R.; Sakamoto, N.; Kunugi, S.; Itoh, M. *Chem. Mater.* **2005**, *17*, 3200.